Unifying finite-temperature dynamical and excited-state quantum phase transitions

Ángel L. Corps [1,2,*] Armando Relaño,[2,3,†] and Jad C. Halimeh [4,5,6,‡]

[1]*Instituto de Estructura de la Materia, IEM-CSIC, Serrano 123, E-28006 Madrid, Spain*

[2]*Grupo Interdisciplinar de Sistemas Complejos (GISC), Universidad Complutense de Madrid, Av. Complutense s/n, E-28040 Madrid, Spain*

[3]*Departamento de Estructura de la Materia, Física Térmica y Electrónica, Universidad Complutense de Madrid, Av. Complutense s/n, E-28040 Madrid, Spain*

[4]*Department of Physics and Arnold Sommerfeld Center for Theoretical Physics (ASC), Ludwig-Maximilians-Universität München, Theresienstraße 37, D-80333 München, Germany*

[5]*Munich Center for Quantum Science and Technology (MCQST), Schellingstraße 4, D-80799 München, Germany*

[6]*Dahlem Center for Complex Quantum Systems, Freie Universität Berlin, 14195 Berlin, Germany*

(Received 29 May 2024; accepted 9 August 2024; published 1 November 2024)

In recent years, various notions of dynamical phase transitions have emerged to describe far-from-equilibrium criticality. A unifying framework connecting these different concepts is still missing, and would provide significant progress toward understanding far-from-equilibrium quantum many-body universality. Initializing our system in a thermal ensemble and subsequently performing quantum quenches in the Lipkin-Meshkov-Glick model, we establish a direct connection between excited-state quantum phase transitions (ESQPTs) and two major types of dynamical phase transitions (DPTs), by relating the phases of the latter to the critical energies and conservation laws in the former. Our work provides further insight into how various concepts of non-ground-state criticality are intimately connected, paving the way for a unified framework of far-from-equilibrium universality.

DOI: 10.1103/PhysRevResearch.6.043080

I. INTRODUCTION

Phase transitions and critical phenomena, along with the resulting features of universality and scaling, are well-understood concepts in equilibrium. In a far-from-equilibrium setting, a unified framework of these notions is still missing. The pursuit of an overarching theory of far-from-equilibrium quantum many-body criticality has recently led to different concepts of nonequilibrium phase transitions [1,2]. The first one is related to the dynamics of the equilibrium Landau order parameter, which is connected to the spontaneous breaking of a global symmetry in the ground state [3]. Upon quenching a given symmetry-broken initial state, if the long-time steady state exhibits a nonzero (zero) order parameter, then the system is in a symmetry-broken (symmetry-preserved) dynamical phase [4,5]. The value of the quench parameter separating these two phases is the dynamical quantum critical point. This type of dynamical phase transition has been dubbed DPT-I, and has been studied in various systems, including mean-field models [6–14], the Hubbard model [15–17], the $O(N)$ model [18–22], and long-range quantum spin chains [23,24], among others [25–27].

Another approach to dynamical criticality encompasses the construction of a dynamical analog of the thermal free energy. This becomes straightforward when recognizing the overlap of the time-evolved wave function with the initial state as a boundary partition function where evolution time stands for a complex inverse temperature [28–30]. By taking the negative of the logarithm of this overlap in the thermodynamic limit, one obtains the return rate, which is the sought-after dynamical analog of the thermal free energy. Nonanalyticities in the return rate are thus dynamical quantum phase transitions (DQPTs) at critical evolution times. DQPTs are also referred to as DPT-II, and have been extensively studied in nonintegrable short-range quantum spin systems [31–33], long-range quantum many-body models [8,9,12,13,24,34–40], topological systems [41–49], higher-dimensional models [42,50–56], systems initialized in thermal ensembles [10,11,57–60], high-energy models known as lattice gauge theories [61–70], non-Hermitian systems [71–76], short-range interacting systems with broken time-translation symmetry [77,78], and disordered models [79,80]. Furthermore, they have been the subject of several successful experiments [81–83].

A different source of criticality beyond the ground state is given by excited-state quantum phase transitions (ESQPTs) [84,85]. They consist in a generalization of quantum phase transitions to excited states, typically manifested as a singularity of the density of states and the level flow. Notwithstanding, the main consequences are dynamical, like huge decoherence [86,87], singularities in quench dynamics [88–92], feedback control in dissipative systems [93], quantum work statistics [94], symmetry-breaking equilibrium states [95,96], dynamical instabilities [97], irreversibility without energy dissipation

*Contact author: corps.angel.l@gmail.com
†Contact author: armando.relano@fis.ucm.es
‡Contact author: jad.halimeh@physik.lmu.de

[98], and reversible quantum information spreading [99]. It has been recently shown that they may give rise to a phase diagram composed by different dynamical phases, each one characterized by a set of (generally noncommuting) constants of motion [12,13,100].

A pertinent question is how these different concepts of nonequilibrium quantum phase transitions are related to one another. When it comes to DPT-I and DPT-II, a connection has been established between the phase of the former and the type of the latter [9]: Starting in a symmetry-broken initial state, if the long-time steady state breaks (preserves) the global symmetry of the quench Hamiltonian, then the DPT-II will be of the anomalous (regular) type. This connection also persists at finite temperature [10,11]. This potentially allows drawing connections between far-from-equilibrium critical exponents arising in both these DPTs [101,102]. Nevertheless, the connection between ESQPTs and DPTs, in particular at finite temperature, is still ambiguous. Given the potential of understanding DPT criticality from that of ESQPTs, it is therefore important to investigate if a direct connection exists. This is the purpose of this Letter.

II. MODEL

Although our arguments are general, we chose a collective model, allowing us to reach large system sizes, as an illustration. It is the transverse-field Ising model with infinite-range interactions, which coincides with a version of the Lipkin-Meshkov-Glick (LMG) Hamiltonian [103–105],

$$\hat{H} = -\frac{\lambda}{N}\hat{J}_x^2 + h\hat{J}_z. \tag{1}$$

The total collective spin operator commutes with the Hamiltonian, $[\hat{H}, \mathbf{J}^2] = 0$, allowing us to separate spin sectors labeled by the eigenvalues of $\mathbf{J}^2$, $j(j+1)$, the dimension of each being $D(j) = 2j+1$. Hamiltonian (1) also has a discrete $\mathbb{Z}_2$ symmetry generated by a π rotation around the z axis. In each j sector it is represented by a parity operator, $\hat{\Pi} = e^{i\pi(\hat{J}_z + j)}$, which allows to classify the Hamiltonian eigenstates according to $\hat{\Pi}|E_{n,\pm}\rangle = \pm|E_{n,\pm}\rangle$, $n = 0, 1, \ldots$.

The full model displays two critical phenomena. At $\lambda_c = \lambda$ there is a quantum phase transition (QPT): for $\lambda > \lambda_c$ the ground state is ferromagnetic and the symmetry generated by $\hat{\Pi}$ is broken; for $\lambda < \lambda_c$ the ground state is symmetric. In the first case, there exists also a thermal phase transition with a critical inverse temperature given by $\beta_c = 2h^{-1}\text{arctanh}(h/\lambda)$; at lower temperatures, the system is ferromagnetic, and the $\mathbb{Z}_2$ symmetry is broken.

To make a connection between these facts and ESQPTs and DPTs, we work with all j sectors, $j = 0, 1, ..., N/2$, each with a degeneracy factor of $g(N, j) = \frac{1+2j}{1+j+N/2}\binom{N}{N/2-j}$, so $\sum_{j=0}^{N/2} g(N, j)D(j) = 2^N$. As noted in [106] for a similar fully connected model, each j sector is completely independent of the others, and therefore it can be described by Hamiltonian (1) with an effective coupling constant given by $\lambda_{\text{eff}} = 2j\lambda/N$. This means that each j sector has its own critical points. For the QPT, it is $\lambda_c(j) = hN/(2j)$. Thus, above the critical point for the global QPT, $\lambda_c = h$, some of the j sectors are in the ferromagnetic ground-state phase, and some others are in the paramagnetic ground-state phase; they are separated at critical value $j_c(\lambda) = Nh/(2\lambda)$. If $j > j_c$, the corresponding sector is in the ferromagnetic phase, and the opposite occurs if $j < j_c$. This argument is important to understand the behavior of ESQPTs.

(i) If $\lambda < \lambda_c$, all the j sectors are in the paramagnetic phase. Therefore, there are no critical energies and their ground-state energies are $\varepsilon_{\text{GS}}(j) = -2hj/N$, where $\varepsilon = 2E/N$.

(ii) If $\lambda > \lambda_c$, the behavior is more involved;

(a) If $j > j_c(\lambda)$, the j sector is in the ferromagnetic ground-state phase. Therefore, it has a critical energy below which all its energy levels are pairwise degenerate in the infinite-size limit. This is the ESQPT energy:

$$\varepsilon_c(j) = -\frac{2hj}{N}. \tag{2}$$

The corresponding ground-state energy is

$$\varepsilon_{\text{GS}}(j) = -\left[2\lambda\left(\frac{j}{N}\right)^2 + \frac{h^2}{2\lambda}\right]. \tag{3}$$

Note that Eqs. (2) and (3) coincide if $j = j_c$, $\varepsilon_c(j_c) = -h^2/\lambda$.

(b) If $j < j_c$, the sector is in the paramagnetic phase. Therefore, none of its eigenlevels are degenerate, with a ground-state energy of $\varepsilon_{\text{GS}}(j) = -2hj/N$.

The main consequence of these facts is that we can define two critical energies for the full Hamiltonian, $\varepsilon_{c1} = -h$ and $\varepsilon_{c2} = -h^2/\lambda > \varepsilon_{c1}$. If $\varepsilon < \varepsilon_{c1}$, all the energy levels are degenerate in pairs; and if $\varepsilon_{c1} \leqslant \varepsilon < \varepsilon_{c2}$, pairwise degenerate and nondegenerate energy occur simultaneously. Above ε_{c2}, there are no degeneracies.

III. EQUIVALENCE OF ESQPTS AND DPTS

All these features refer to static or equilibrium properties of the LMG Hamiltonian. However, DPTs are nonequilibrium phenomena. To establish a link between them, we focus on a dynamical property of a class of ESQPTs. In Refs. [12,13,100] it is shown that for a wide class of models to which the LMG belongs, there are two additional constants of motion below the critical energy of the ESQPT related to the order parameter of the QPT and the operator generating the $\mathbb{Z}_2$ symmetry: $\hat{\mathcal{C}} = \text{sign}(\hat{J}_x)$ and $\hat{\mathcal{K}} = (i/2)[\hat{\mathcal{C}}, \hat{\Pi}]$. Thus, if a nonequilibrium protocol leads the system into an energy region below the ESQPT, then the dynamics is restricted by the conservation of $\hat{\mathcal{C}}$ and $\hat{\mathcal{K}}$. As a consequence, quenching an initial symmetry-breaking state polarized along the ferromagnetic axis cannot lead the order parameter $\langle\hat{J}_x\rangle$ to change sign in its dynamics. On the contrary, there are no restrictions if the energy is above the ESQPT. These dynamical features are also expected for noncollective models with an equilibrium symmetry-breaking phase [13,107].

From these facts, we propose the main conclusion of this Letter: there are only two possible dynamical phases (DPs) starting from an equilibrium symmetry-breaking initial state:

DPa. A constant value for $\hat{\mathcal{C}}$ and $\hat{\mathcal{K}}$, together with the order parameter $\langle\hat{J}_x\rangle$ oscillating around a nonzero value, without changing sign.

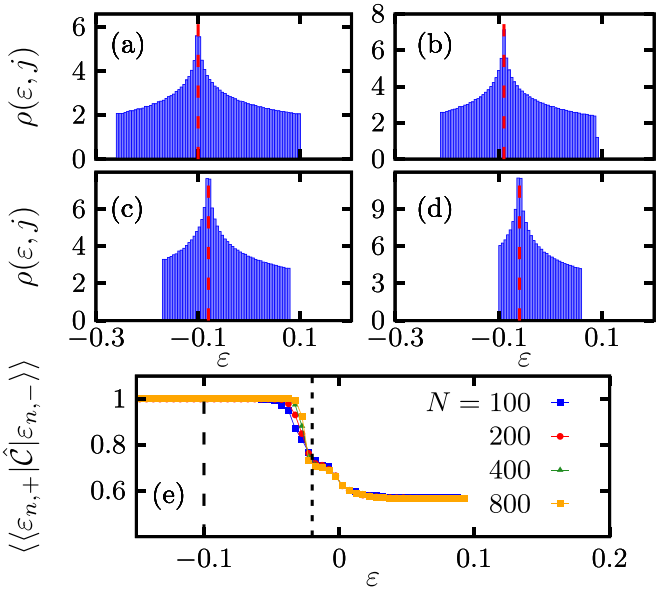

FIG. 1. (a)–(d) Density of states for the LMG model with $N = 10\,000$ particles and parameters $h = 0.1$, $\lambda = 0.5$. Each panel corresponds to the level density as obtained for a given j sector. (a) $j = N/2 = 5000$, (b) $j = 4500$, (c) $j = 4000$, (d) $j = 3000$. The eigenvalues are rescaled as $\varepsilon = 2E/N$. Black vertical lines mark the ESQPT critical energy of each j sector (2). (e) Expectation value of $\hat{\mathcal{C}}$ in states of different parity as a function of energy. Model parameters are $h = 0.1$, $\lambda = 0.5$, with N as indicated in the panel. Dashed vertical lines mark the energies $\varepsilon = -h = -0.1$ and $\varepsilon = -h^2/\lambda = -0.02$. Points represent an average over a small energy window containing all j sectors, and with the corresponding degeneracy factors $g(N, j)$ appropriately taken into account.

DPb. Both $\hat{\mathcal{C}}$, $\hat{\mathcal{K}}$, and $\langle \hat{J}_x \rangle$ oscillating around zero. These two dynamical phases are separated by the critical energy of the ESQPT.

To illustrate this picture, we show in Fig. 1 the density of states for $\lambda = 0.5$, $h = 0.1$, and different values of j. All of them verify $j > j_c(\lambda)$, and therefore exhibit ESQPTs. It is clearly seen that the corresponding critical energy, identified by the logarithmic divergence in the density of states, shifts to lower energies as j is increased. This means that the populated sectors of j play a fundamental role in the dynamics. Let us suppose that we prepare a state with $\epsilon = -0.07$. This value is above the critical energy of panels (a)–(c), and below the one on panel (d). If the expectation value of $\mathbf{J}^2$ in our state, which is a conserved quantity, is narrowly picked around $j/N > 0.35$, then neither $\hat{\mathcal{C}}$ nor $\hat{\mathcal{K}}$ are constants, and therefore the order parameter $\langle J_x \rangle$ must oscillate around zero. On the contrary, from Eqs. (2) and (3), we can conclude that if $\sqrt{0.06} < j/N < 0.35$, then both $\hat{\mathcal{C}}$ and $\hat{\mathcal{K}}$ are constant, and therefore $\langle \hat{J}_x \rangle$ cannot cross $\langle \hat{J}_x \rangle = 0$.

In Fig. 1(e) we represent the consequences of the previous facts for the full Hamiltonian. As discussed in [100], the constancy of $\hat{\mathcal{C}}$ requires that $\langle \varepsilon_{n,-}|\hat{\mathcal{C}}|\varepsilon_{n,+}\rangle = \pm 1$ for degenerate energy levels $\varepsilon_{n,-} = \varepsilon_{n,+}$. The results indicate that this is globally fulfilled if $\varepsilon < \varepsilon_{c2}$ in the thermodynamic limit. The reason is that, the lower the value of j, the larger the degeneracy factor, $g(N, j)$; therefore, only the lowest possible value of j, which gives rise to the highest critical energy $\varepsilon_c(j)$, contributes to the dynamics of $\hat{\mathcal{C}}$ in the thermodynamic limit. Therefore, we can expect symmetry-broken thermal states if $\varepsilon < \varepsilon_{c2}$, whose associated temperature is below the critical temperature of the phase transition, $T < T_c$. However, this is not enough to determine the dynamics of a thermal state subjected to a nonequilibrium process. As $\hat{\mathbf{J}}^2$ is conserved, the population of each j sector must be taken into account to determine whether the final state is above or below the critical energies of the corresponding ESQPTs. It is worth noting that the same qualitative result shown in Fig. 1(e) has been observed in the transverse-field Ising model with long-range interactions [13], in which $\hat{\mathbf{J}}^2$ is not conserved. Hence, the same classification in two dynamical phases is expected for noncollective models.

To test our hypothesis, we have performed a set of numerical experiments on the LMG model. In all of them, we prepare an initial state in the ferromagnetic phase, with $\varepsilon < \varepsilon_{c1}$. As $\hat{\mathbf{J}}^2$, $\hat{\Pi}$, $\hat{\mathcal{C}}$, $\hat{\mathcal{K}}$ are conserved under these circumstances, the most general equilibrium state is

$$\hat{\rho} = \frac{1}{Z} e^{-\beta \hat{H} - \mu_c \hat{\mathcal{C}} - \mu_k \hat{\mathcal{K}} - \mu_\pi \hat{\Pi} - \mu_j \hat{\mathbf{J}}^2}, \tag{4}$$

where Z is the partition function ensuring that $\mathrm{Tr}[\hat{\rho}] = 1$, and μ_c, μ_k, μ_π, $\mu_j \in \mathbb{R}$ are free parameters linked to the initial values of $\langle \hat{\mathcal{C}} \rangle$, $\langle \hat{\mathcal{K}} \rangle$, $\langle \hat{\Pi} \rangle$, and $\langle \hat{\mathbf{J}}^2 \rangle$. To study the dynamics, we start from an initial state $\hat{\rho}_i$ of the form (4) with $\mu_k = \mu_\pi = \mu_j = 0$, $\mu_c = 100$, and $\beta = 5$, though our conclusions also hold for other values (see the Appendix). The initial Hamiltonian, $\hat{H}_i$, has parameters $\lambda = 0.5$ and $h_i = 0$. This choice gives rise to a polarized thermal state, with $\langle \hat{J}_x \rangle < 0$. We then quench the initial state with a final Hamiltonian, $\hat{H}_f$, with different $h_f = 0.1, 0.15, 0.2, 0.3$ and $\lambda = 0.5$. The time-evolved density operator at time t is $\hat{\rho}_f(t) = e^{-i\hat{H}_f t}\hat{\rho}_i e^{i\hat{H}_f t}$. Since $\hat{\mathbf{J}}^2$ is conserved by Eq. (1), the distribution $P(j)$ of populated j sectors remains unchanged in the wake of the quench. The dynamics will be dominated by j sectors with large $P(j)$.

Figure 2 illustrates the dynamical effects of these quenches. We focus first on the largest system size, $N = 1600$. For $h_f = 0.1$ and $h_f = 0.15$, the average quench energy is below the critical energy of the most-populated j sector. We can see that $\langle \hat{J}_x \rangle$ oscillates around a nonzero value (note that the larger the system, the longer the oscillating behavior remains), and $\langle \hat{\mathcal{C}} \rangle$ is perfectly constant; therefore, the system is in the dynamical phase DPa. On the contrary, for $h_f = 0.2$ and $h_f = 0.3$ the average quench energy is above the critical one, and the dynamics is consistent with the dynamical phase DPb: both $\langle \hat{J}_x \rangle$ and $\langle \hat{\mathcal{C}} \rangle$ oscillate around zero. It is worth to remark that the critical quench separating regular and anomalous DPTs-II is given by $h_f^c \approx 0.1776$ [10]. Therefore, our numerical results show that DPa leads to anomalous DPTs-II, and DPb to regular ones.

Notwithstanding, the picture is not so clear for smaller system sizes. For $h_f = 0.15$ and $N = 100$, 200, 400, and 800, $\langle \hat{J}_x \rangle$ oscillates around a nonzero value, but $\langle \hat{\mathcal{C}} \rangle$ is clearly not constant. To explain this behavior and to understand what is expected to occur in the thermodynamic limit (TL), we perform a finite-size scaling. Results are given in Table I. We focus there on two quantities: the energy width, $\sigma_\varepsilon =$

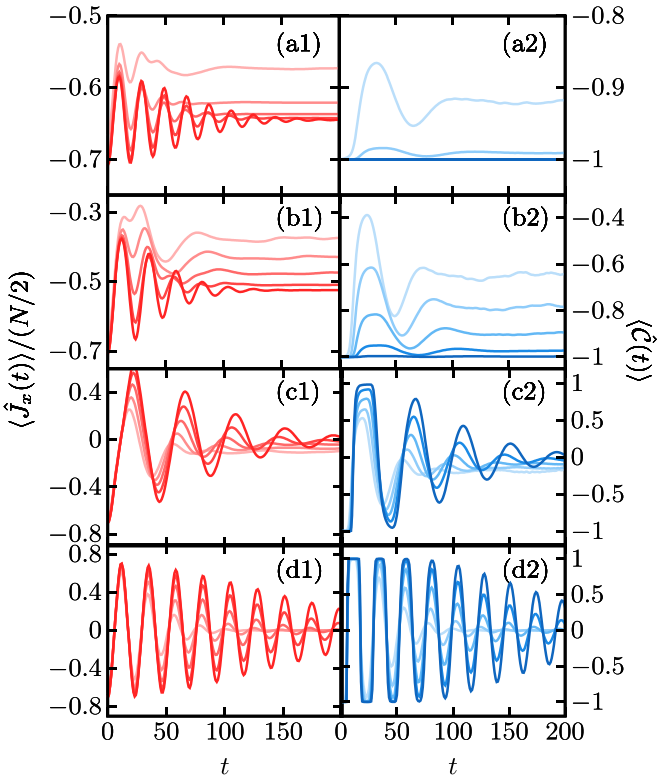

FIG. 2. Instantaneous values of the magnetization, $\hat{J}_x$, (left), and the $\hat{C}$ operator, (right), following different quenches with $\beta = 5$, $\lambda = 0.5$ and $h_i = 0$. (a1,2) $h_f = 0.1$; (b1,2) $h_f = 0.15$; (c1,2) $h_f = 0.2$; (d1,2) $h_f = 0.3$. System sizes are $N = 100, 200, 400, 800, 1600$ from light to dark color curves. In all the cases, $\langle\varepsilon\rangle = -0.126$ and the critical energies for the most populated j-sector, given by Eq. (2), are: (a1,2) $\varepsilon_c(j_{\max}) = -0.0711$, (b1,2) $\varepsilon_c(j_{\max}) = -0.107$, (c1,2) $\varepsilon_c(j_{\max}) = -0.142$, (d1,2) $\varepsilon_c(j_{\max}) = -0.213$.

$\sqrt{\langle\hat{H}^2\rangle - \langle\hat{H}\rangle^2}$, and a range of critical energies obtained from the population of the different j sectors (see caption for details). The key point is the overlap between these two intervals. For a nonempty overlap, we expect a mixture of DPa and DPb. For those sectors in which $\langle\varepsilon\rangle_j < \varepsilon_c(j)$, $\langle\hat{C}\rangle_j$ is constant, and $\langle\hat{J}_x\rangle_j$ oscillates around a nonzero value [$\langle\bullet\rangle_j$ stands for the expectation value of an observable in the projection of the state onto the eigenspace in which $\hat{\mathbf{J}}^2$ is equal to $j(j+1)$]. And for those sectors in which $\langle\varepsilon\rangle_j > \varepsilon_c(j)$, both $\langle\hat{C}\rangle_j$ and $\langle\hat{J}_x\rangle_j$ oscillate around zero. Therefore, when putting together all the j sectors, we obtain the intermediate picture observed for $h_f = 0.15$ and $N = 100$, 200, 400, and 800. On the contrary, if the intervals do not overlap, the dynamical phases are either DPa or DPb.

To extrapolate these result to the TL, we study how the energy width and the range of critical energies change with system size. A least-squares fit of the data shown in Table I provides $\sigma_\varepsilon \propto N^{-0.516(5)}$ and $|\varepsilon_{c,\max} - \varepsilon_{c,\min}| \propto N^{-0.54(2)}$. This means that the only possible nonequilibrium dynamics in the TL is either DPa or DPb, and that an initial state gives rise to either one or the other depending on whether its average quench energy is below or above the critical energy of the ESQPT.

TABLE I. Average energy, $\langle\varepsilon\rangle$, width σ_ε and estimated maximal and minimal critical energies corresponding to the minimum and maximum j-sectors, respectively, with a cumulative probability of 95%, as a function of the system size N for the quench $h_i = 0 \to h_f = 0.15$, $\lambda = 0.5$.

N	$\langle\varepsilon\rangle \pm \sigma_\varepsilon$	$[\varepsilon_{c,\min}, \varepsilon_{c,\max}]$
100	-0.120 ± 0.041	$[-0.135, -0.057]$
200	-0.124 ± 0.028	$[-0.1275, -0.078]$
400	-0.125 ± 0.020	$[-0.1223, -0.08775]$
800	-0.126 ± 0.014	$[-0.1178, -0.09375]$
1600	-0.1259 ± 0.0097	$[-0.1146, -0.09769]$

IV. DISCUSSION AND OUTLOOK

Through analytic arguments and numerical simulations, we have shown that ESQPTs and two major types of DPTs have a direct connection to each other in the LMG model. When the quench energy is below (above) the ESQPT critical points, the long-time steady-state falls in the ferromagnetic (paramagnetic) phase of DPT-I. Given that DPT-I and DPT-II have been shown to be directly connected to each other in the LMG model [9,10], this means that ESQPTs are also directly connected to DPT-II.

Demonstrating such a direct connection between ESQPTs and DPTs provides evidence that varying concepts of criticality beyond that of the ground state may be intimately related. This is promising in the pursuit of an overarching framework for far-from-equilibrium quantum many-body universality.

Our conclusions should be valid in other mean-field models where large enough system sizes are accessible in order to faithfully probe criticality. An interesting question is whether our findings also hold for nonintegrable models where access to the full spectrum is only possible for small system sizes that cannot reasonably discern criticality. This makes it hard to adequately study ESQPTs in such systems, although a direct connection between DPT-I and DPT-II is well established in them [108].

Another interesting venue for future work entails connecting the critical exponents extracted from ESQPTs and DPTs. For example, it is known that DPT-I and DPT-II have seemingly disparate critical exponents, but since both DPTs have been shown to coincide [10,108], it is likely that their critical exponents have a direct relation.

TABLE II. Average energy, $\langle\varepsilon\rangle$, of the quenched state $h_i = 0 \to h_f$, for different values of h_f, and estimated maximal and minimal critical energies corresponding to the minimum and maximum j sectors, respectively, with a cumulative probability of 95%. System size is $N = 1600$ and $\beta = 10$.

Quench	$\langle\varepsilon\rangle$	$[\varepsilon_{c,\min}, \varepsilon_{c,\max}]$
$h_f = 0.2$	-0.2430 ± 0.0063	$[-0.1988, -0.1955]$
$h_f = 0.24$	-0.2430 ± 0.0063	$[-0.2385, -0.2346]$
$h_f = 0.26$	-0.2430 ± 0.0063	$[-0.2584, -0.2542]$
$h_f = 0.3$	-0.2430 ± 0.0063	$[-0.2981, -0.2933]$

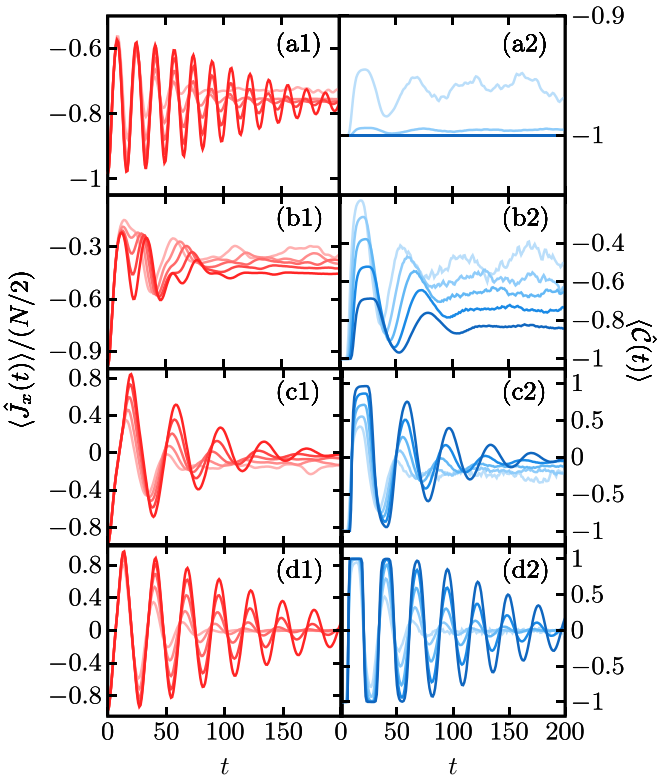

FIG. 3. Instantaneous values of the magnetization, $\hat{J}_x$, (left), and the $\hat{C}$ operator, (right), following different quenches with $\beta = 10$, $\lambda = 0.5$, and $h_i = 0$. (a1,2) $h_f = 0.2$; (b1,2) $h_f = 0.24$; (c1,2) $h_f = 0.26$; (d1,2) $h_f = 0.3$. System sizes are $N = 100, 200, 400, 800, 1600$ from light to dark color curves. The critical $h_f^c \approx 0.2464$.

ACKNOWLEDGMENTS

A.L.C. and A.R. acknowledge financial support by the Spanish Grants No. PGC-2018-094180-B-I00, No. PID2019-106820RB-C21, and No. PID2022-136285NB-C31, funded by the Ministerio de Ciencia e Innovación/Agencia Estatal de Investigación MCIN/AEI/10.13039/501100011033 and FEDER "A Way of Making Europe." A.L.C. acknowledges financial support from "la Caixa" Foundation (ID 100010434) through the fellowship LCF/BQ/DR21/11880024. J.C.H. acknowledges financial support through the Emmy Noether Programme of the German Research Foundation (DFG) under Grant No. HA 8206/1-1.

TABLE III. Average energy, $\langle\varepsilon\rangle$, of the quenched state $h_i = 0 \to h_f$, for different values of h_f, and estimated maximal and minimal critical energies corresponding to the minimum and maximum j sectors, respectively, with a cumulative probability of 95%. System size is $N = 1600$ and $\beta = 7$.

Quench	$\langle\varepsilon\rangle$	$[\varepsilon_{c,\min}, \varepsilon_{c,\max}]$
$h_f = 0.15$	-0.2136 ± 0.0094	$[-0.1418, -0.1354]$
$h_f = 0.21$	-0.2136 ± 0.0094	$[-0.1985, -0.1895]$
$h_f = 0.26$	-0.2136 ± 0.0094	$[-0.2457, -0.2347]$
$h_f = 0.33$	-0.2136 ± 0.0094	$[-0.3119, -0.2978]$

TABLE IV. Average energy, $\langle\varepsilon\rangle$, of the quenched state $h_i = 0 \to h_f$, for different values of h_f, and estimated maximal and minimal critical energies corresponding to the minimum and maximum j sectors, respectively, with a cumulative probability of 95%. System size is $N = 1600$ and $\beta = 4.5$.

Quench	$\langle\varepsilon\rangle$	$[\varepsilon_{c,\min}, \varepsilon_{c,\max}]$
$h_f = 0.08$	-0.07522 ± 0.01108	$[-0.0507, -0.0363]$
$h_f = 0.12$	-0.07522 ± 0.01108	$[-0.07605, -0.0545]$
$h_f = 0.15$	-0.07522 ± 0.01108	$[-0.09506, -0.06806]$
$h_f = 0.18$	-0.07522 ± 0.01108	$[-0.1141, -0.08168]$

APPENDIX: ADDITIONAL NUMERICAL RESULTS

Here we show the quench dynamics generated by initial states with inverse temperatures β and h_f different from those in the main text. The qualitative picture for $\beta = 10, 7,$ and 4.5 in Figs. 3–5 is essentially the same as in Fig. 2. As an exception to this behavior, in Fig. 6 we focus on $\beta = 3.5 < \beta_c$, for which the time evolution of the relevant observables always oscillates around zero, irrespective of h_f. This is because for $\beta < \beta_c$, the most populated j-sector is always below the critical j_c, and therefore there is no ESQPT critical energy. As such, this does not contradict our conclusions, but rather reinforces them, because also for $\beta < \beta_c$ there is

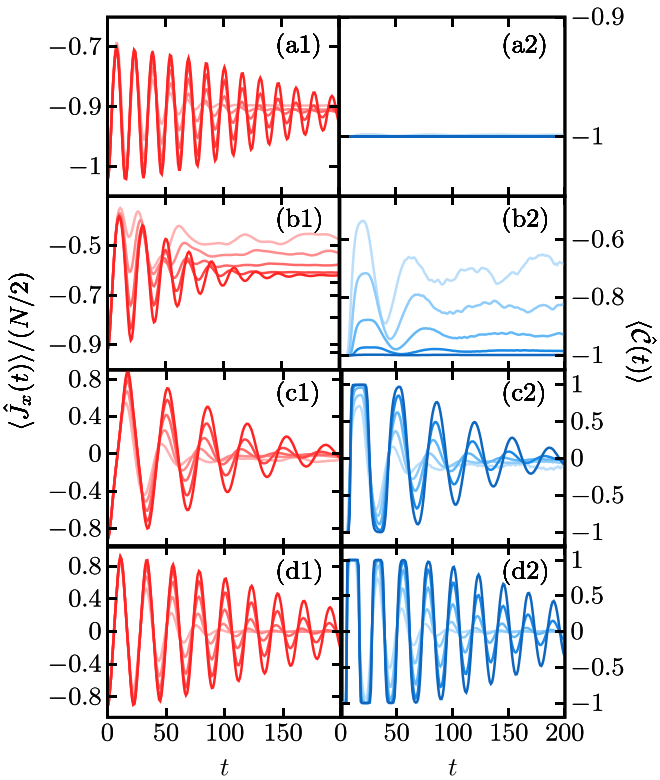

FIG. 4. Instantaneous values of the magnetization, $\hat{J}_x$, (left), and the $\hat{C}$ operator, (right), following different quenches with $\beta = 7$, $\lambda = 0.5$, and $h_i = 0$. (a1,2) $h_f = 0.15$; (b1,2) $h_f = 0.21$; (c1,2) $h_f = 0.26$; (d1,2) $h_f = 0.33$. System sizes are $N = 100, 200, 400, 800, 1600$ from light to dark color curves. The critical $h_f^c \approx 0.2311$.

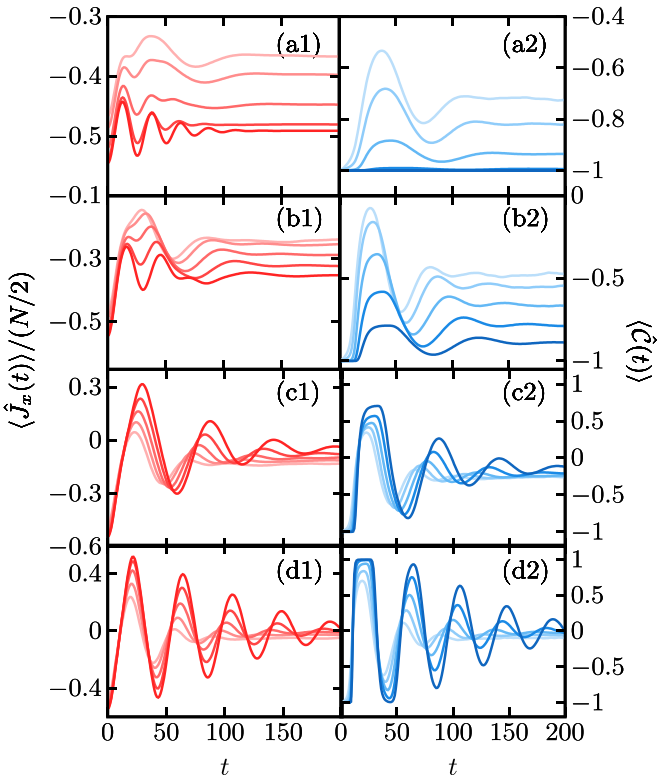

FIG. 5. Instantaneous values of the magnetization, $\hat{J}_x$, (left), and the $\hat{\mathcal{C}}$ operator, (right), following different quenches with $\beta = 4.5$, $\lambda = 0.5$, and $h_i = 0$. (a1,2) $h_f = 0.08$; (b1,2) $h_f = 0.12$; (c1,2) $h_f = 0.15$; (d1,2) $h_f = 0.18$. System sizes are $N = 100, 200, 400, 800, 1600$ from light to dark color curves. The critical $h_f^c \approx 0.1378$.

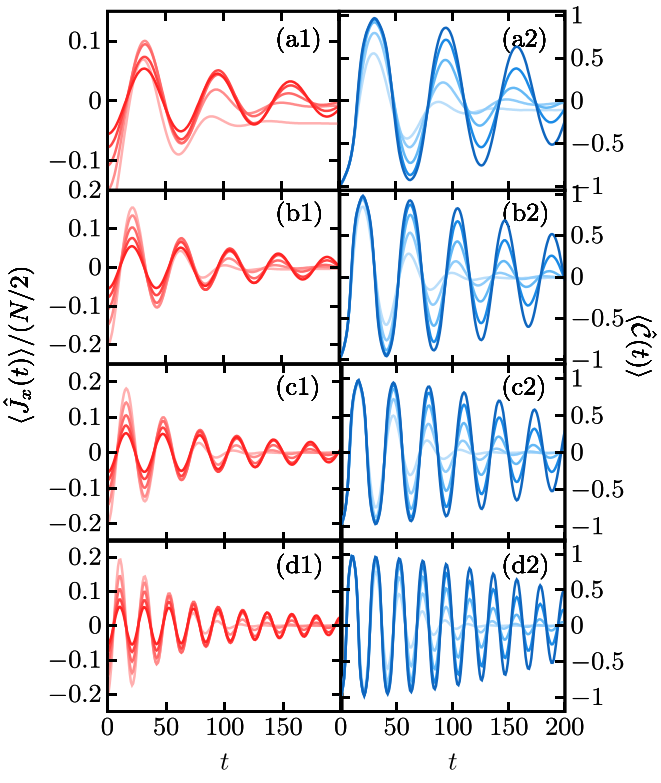

FIG. 6. Instantaneous values of the magnetization, $\hat{J}_x$, (left), and the $\hat{\mathcal{C}}$ operator, (right), following different quenches with $\beta = 3.5$, $\lambda = 0.5$, and $h_i = 0$. (a1,2) $h_f = 0.1$; (b1,2) $h_f = 0.15$; (c1,2) $h_f = 0.2$; (d1,2) $h_f = 0.3$. System sizes are $N = 100, 200, 400, 800, 1600$ from light to dark color curves. Note that as N increases, the oscillation in $\langle \hat{J}_x(t)\rangle$ gives an average value that approaches zero. Since our state is prepared with $h_i = 0$, in the infinite-N limit, the magnetization should vanish at all times. Finite-size deviations from this limiting behavior are expected.

no DPT for quenches in h. Tables II, III, and IV compare the average energy of the quenched state with the range of ESQPT critical energies associated to the 95% most populated j sectors in the final Hamiltonian. Note that for the quench where $\beta < \beta_c$, Fig. 6 has no corresponding table as there is no ESQPT critical energy.

[1] T. Mori, T. N. Ikeda, E. Kaminishi, and M. Ueda, Thermalization and prethermalization in isolated quantum systems: A theoretical overview, J. Phys. B **51**, 112001 (2018).

[2] M. Heyl, Dynamical quantum phase transitions: A review, Rep. Prog. Phys. **81**, 054001 (2018).

[3] J. Cardy, *Scaling and Renormalization in Statistical Physics*, Cambridge Lecture Notes in Physics (Cambridge University Press, Cambridge, England, 1996).

[4] M. Moeckel and S. Kehrein, Interaction quench in the Hubbard model, Phys. Rev. Lett. **100**, 175702 (2008).

[5] M. Eckstein and M. Kollar, Nonthermal steady states after an interaction quench in the Falicov-Kimball model, Phys. Rev. Lett. **100**, 120404 (2008).

[6] B. Sciolla and G. Biroli, Quantum quenches and off-equilibrium dynamical transition in the infinite-dimensional Bose-Hubbard model, Phys. Rev. Lett. **105**, 220401 (2010).

[7] B. Sciolla and G. Biroli, Dynamical transitions and quantum quenches in mean-field models, J. Stat. Mech. (2011) P11003.

[8] B. žunkovič, A. Silva, and M. Fabrizio, Dynamical phase transitions and Loschmidt echo in the infinite-range xy model, Philos. Trans. R. Soc. A **374**, 20150160 (2016).

[9] I. Homrighausen, N. O. Abeling, V. Zauner-Stauber, and J. C. Halimeh, Anomalous dynamical phase in quantum spin chains with long-range interactions, Phys. Rev. B **96**, 104436 (2017).

[10] J. Lang, B. Frank, and J. C. Halimeh, Concurrence of dynamical phase transitions at finite temperature in the fully connected transverse-field Ising model, Phys. Rev. B **97**, 174401 (2018).

[11] J. Lang, B. Frank, and J. C. Halimeh, Dynamical quantum phase transitions: A geometric picture, Phys. Rev. Lett. **121**, 130603 (2018).

[12] Á. L. Corps and A. Relaño, Dynamical and excited-state quantum phase transitions in collective systems, Phys. Rev. B **106**, 024311 (2022).

[13] Á. L. Corps and A. Relaño, Theory of dynamical phase transitions in quantum systems with symmetry-breaking eigenstates, Phys. Rev. Lett. **130**, 100402 (2023).

[14] Á. L. Corps, P. Pérez-Fernández, and A. Relaño, Relaxation time as a control parameter for exploring dynamical phase diagrams, Phys. Rev. B **108**, 174305 (2023).

[15] M. Eckstein, M. Kollar, and P. Werner, Thermalization after an interaction quench in the Hubbard model, Phys. Rev. Lett. **103**, 056403 (2009).

[16] M. Moeckel and S. Kehrein, Crossover from adiabatic to sudden interaction quenches in the Hubbard model: Prethermalization and non-equilibrium dynamics, New J. Phys. **12**, 055016 (2010).

[17] N. Tsuji, M. Eckstein, and P. Werner, Nonthermal antiferromagnetic order and nonequilibrium criticality in the Hubbard model, Phys. Rev. Lett. **110**, 136404 (2013).

[18] A. Chandran, A. Nanduri, S. S. Gubser, and S. L. Sondhi, Equilibration and coarsening in the quantum $o(n)$ model at infinite n, Phys. Rev. B **88**, 024306 (2013).

[19] A. Maraga, A. Chiocchetta, A. Mitra, and A. Gambassi, Aging and coarsening in isolated quantum systems after a quench: Exact results for the quantum O(n) model with $n \to \infty$, Phys. Rev. E **92**, 042151 (2015).

[20] P. Smacchia, M. Knap, E. Demler, and A. Silva, Exploring dynamical phase transitions and prethermalization with quantum noise of excitations, Phys. Rev. B **91**, 205136 (2015).

[21] A. Chiocchetta, A. Gambassi, S. Diehl, and J. Marino, Dynamical crossovers in prethermal critical states, Phys. Rev. Lett. **118**, 135701 (2017).

[22] J. C. Halimeh and M. F. Maghrebi, Quantum aging and dynamical universality in the long-range $o(n \to \infty)$ model, Phys. Rev. E **103**, 052142 (2021).

[23] J. C. Halimeh, V. Zauner-Stauber, I. P. McCulloch, I. de Vega, U. Schollwöck, and M. Kastner, Prethermalization and persistent order in the absence of a thermal phase transition, Phys. Rev. B **95**, 024302 (2017).

[24] B. Žunkovič, M. Heyl, M. Knap, and A. Silva, Dynamical quantum phase transitions in spin chains with long-range interactions: Merging different concepts of nonequilibrium criticality, Phys. Rev. Lett. **120**, 130601 (2018).

[25] A. Gambassi and P. Calabrese, Quantum quenches as classical critical films, Europhys. Lett. **95**, 66007 (2011).

[26] T. Langen, T. Gasenzer, and J. Schmiedmayer, Prethermalization and universal dynamics in near-integrable quantum systems, J. Stat. Mech. (2016) 064009.

[27] M. Marcuzzi, J. Marino, A. Gambassi, and A. Silva, Prethermalization from a low-density Holstein-Primakoff expansion, Phys. Rev. B **94**, 214304 (2016).

[28] M. Heyl, A. Polkovnikov, and S. Kehrein, Dynamical quantum phase transitions in the transverse-field Ising model, Phys. Rev. Lett. **110**, 135704 (2013).

[29] M. Heyl, Dynamical quantum phase transitions in systems with broken-symmetry phases, Phys. Rev. Lett. **113**, 205701 (2014).

[30] M. Heyl, Scaling and universality at dynamical quantum phase transitions, Phys. Rev. Lett. **115**, 140602 (2015).

[31] C. Karrasch and D. Schuricht, Dynamical phase transitions after quenches in nonintegrable models, Phys. Rev. B **87**, 195104 (2013).

[32] S. Vajna and B. Dóra, Disentangling dynamical phase transitions from equilibrium phase transitions, Phys. Rev. B **89**, 161105(R) (2014).

[33] F. Andraschko and J. Sirker, Dynamical quantum phase transitions and the Loschmidt echo: A transfer matrix approach, Phys. Rev. B **89**, 125120 (2014).

[34] J. C. Halimeh and V. Zauner-Stauber, Dynamical phase diagram of quantum spin chains with long-range interactions, Phys. Rev. B **96**, 134427 (2017).

[35] V. Zauner-Stauber and J. C. Halimeh, Probing the anomalous dynamical phase in long-range quantum spin chains through Fisher-zero lines, Phys. Rev. E **96**, 062118 (2017).

[36] N. Defenu, T. Enss, and J. C. Halimeh, Dynamical criticality and domain-wall coupling in long-range hamiltonians, Phys. Rev. B **100**, 014434 (2019).

[37] P. Uhrich, N. Defenu, R. Jafari, and J. C. Halimeh, Out-of-equilibrium phase diagram of long-range superconductors, Phys. Rev. B **101**, 245148 (2020).

[38] J. C. Halimeh, M. Van Damme, L. Guo, J. Lang, and P. Hauke, Dynamical phase transitions in quantum spin models with antiferromagnetic long-range interactions, Phys. Rev. B **104**, 115133 (2021).

[39] A. Mitra, T. Albash, P. D. Blocher, J. Takahashi, A. Miyake, G. W. Biedermann, and I. H. Deutsch, Macrostates vs. microstates in the classical simulation of critical phenomena in quench dynamics of 1d Ising models, arXiv:2310.08567.

[40] Á. L. Corps, P. Stránský, and P. Cejnar, Mechanism of dynamical phase transitions: The complex-time survival amplitude, Phys. Rev. B **107**, 094307 (2023).

[41] S. Vajna and B. Dóra, Topological classification of dynamical phase transitions, Phys. Rev. B **91**, 155127 (2015).

[42] M. Schmitt and S. Kehrein, Dynamical quantum phase transitions in the kitaev honeycomb model, Phys. Rev. B **92**, 075114 (2015).

[43] N. Sedlmayr, P. Jaeger, M. Maiti, and J. Sirker, Bulk-boundary correspondence for dynamical phase transitions in one-dimensional topological insulators and superconductors, Phys. Rev. B **97**, 064304 (2018).

[44] I. Hagymási, C. Hubig, Ö. Legeza, and U. Schollwöck, Dynamical topological quantum phase transitions in nonintegrable models, Phys. Rev. Lett. **122**, 250601 (2019).

[45] T. Masłowski and N. Sedlmayr, Quasiperiodic dynamical quantum phase transitions in multiband topological insulators and connections with entanglement entropy and fidelity susceptibility, Phys. Rev. B **101**, 014301 (2020).

[46] S. Porta, F. Cavaliere, M. Sassetti, and N. Traverso Ziani, Topological classification of dynamical quantum phase transitions in the xy chain, Sci. Rep. **10**, 12766 (2020).

[47] R. Okugawa, H. Oshiyama, and M. Ohzeki, Mirror-symmetry-protected dynamical quantum phase transitions in topological crystalline insulators, Phys. Rev. Res. **3**, 043064 (2021).

[48] K. Wrześniewski, I. Weymann, N. Sedlmayr, and T. Domański, Dynamical quantum phase transitions in a mesoscopic superconducting system, Phys. Rev. B **105**, 094514 (2022).

[49] T. Masłowski and N. Sedlmayr, Dynamical bulk-boundary correspondence and dynamical quantum phase transitions in higher-order topological insulators, Phys. Rev. B **108**, 094306 (2023).

[50] U. Bhattacharya and A. Dutta, Emergent topology and dynamical quantum phase transitions in two-dimensional closed quantum systems, Phys. Rev. B **96**, 014302 (2017).

[51] S. A. Weidinger, M. Heyl, A. Silva, and M. Knap, Dynamical quantum phase transitions in systems with continuous symmetry breaking, Phys. Rev. B **96**, 134313 (2017).

[52] M. Heyl, F. Pollmann, and B. Dóra, Detecting equilibrium and dynamical quantum phase transitions in Ising chains via out-of-time-ordered correlators, Phys. Rev. Lett. **121**, 016801 (2018).

[53] S. D. Nicola, B. Doyon, and M. J. Bhaseen, Stochastic approach to non-equilibrium quantum spin systems, J. Phys. A: Math. Theor. **52**, 05LT02 (2019).

[54] T. Hashizume, I. P. McCulloch, and J. C. Halimeh, Dynamical phase transitions in the two-dimensional transverse-field Ising model, Phys. Rev. Res. **4**, 013250 (2022).

[55] T. Hashizume, J. C. Halimeh, and I. P. McCulloch, Hybrid infinite time-evolving block decimation algorithm for long-range multidimensional quantum many-body systems, Phys. Rev. B **102**, 035115 (2020).

[56] A. Kosior and M. Heyl, Vortex loop dynamics and dynamical quantum phase transitions in 3d fermion matter, Phys. Rev. B **109**, L140303 (2024).

[57] N. O. Abeling and S. Kehrein, Quantum quench dynamics in the transverse field Ising model at nonzero temperatures, Phys. Rev. B **93**, 104302 (2016).

[58] U. Bhattacharya, S. Bandyopadhyay, and A. Dutta, Mixed state dynamical quantum phase transitions, Phys. Rev. B **96**, 180303(R) (2017).

[59] M. Heyl and J. C. Budich, Dynamical topological quantum phase transitions for mixed states, Phys. Rev. B **96**, 180304(R) (2017).

[60] N. Sedlmayr, M. Fleischhauer, and J. Sirker, Fate of dynamical phase transitions at finite temperatures and in open systems, Phys. Rev. B **97**, 045147 (2018).

[61] T. V. Zache, N. Mueller, J. T. Schneider, F. Jendrzejewski, J. Berges, and P. Hauke, Dynamical topological transitions in the massive schwinger model with a θ term, Phys. Rev. Lett. **122**, 050403 (2019).

[62] Y.-P. Huang, D. Banerjee, and M. Heyl, Dynamical quantum phase transitions in u(1) quantum link models, Phys. Rev. Lett. **122**, 250401 (2019).

[63] S. P. Pedersen and N. T. Zinner, Lattice gauge theory and dynamical quantum phase transitions using noisy intermediate-scale quantum devices, Phys. Rev. B **103**, 235103 (2021).

[64] R. B. Jensen, S. P. Pedersen, and N. T. Zinner, Dynamical quantum phase transitions in a noisy lattice gauge theory, Phys. Rev. B **105**, 224309 (2022).

[65] J. C. Halimeh, M. V. Damme, T. V. Zache, D. Banerjee, and P. Hauke, Achieving the quantum field theory limit in far-from-equilibrium quantum link models, Quantum **6**, 878 (2022).

[66] M. Van Damme, T. V. Zache, D. Banerjee, P. Hauke, and J. C. Halimeh, Dynamical quantum phase transitions in spin-$su(1)$ quantum link models, Phys. Rev. B **106**, 245110 (2022).

[67] N. Mueller, J. A. Carolan, A. Connelly, Z. Davoudi, E. F. Dumitrescu, and K. Yeter-Aydeniz, Quantum computation of dynamical quantum phase transitions and entanglement tomography in a lattice gauge theory, PRX Quantum **4**, 030323 (2023).

[68] D. Pomarico, L. Cosmai, P. Facchi, C. Lupo, S. Pascazio, and F. V. Pepe, Dynamical quantum phase transitions of the schwinger model: Real-time dynamics on IBM quantum, Entropy **25**, 608 (2023).

[69] M. Van Damme, J.-Y. Desaules, Z. Papić, and J. C. Halimeh, Anatomy of dynamical quantum phase transitions, Phys. Rev. Res. **5**, 033090 (2023).

[70] J. Osborne, I. P. McCulloch, and J. C. Halimeh, Probing confinement through dynamical quantum phase transitions: From quantum spin models to lattice gauge theories, arXiv:2310.12210.

[71] L. Zhou, Q.-H. Wang, H. Wang, and J. Gong, Dynamical quantum phase transitions in non-Hermitian lattices, Phys. Rev. A **98**, 022129 (2018).

[72] L. Zhou and Q. Du, Non-Hermitian topological phases and dynamical quantum phase transitions: A generic connection, New J. Phys. **23**, 063041 (2021).

[73] R. Hamazaki, Exceptional dynamical quantum phase transitions in periodically driven systems, Nat. Commun. **12**, 5108 (2021).

[74] D. Mondal and T. Nag, Anomaly in the dynamical quantum phase transition in a non-Hermitian system with extended gapless phases, Phys. Rev. B **106**, 054308 (2022).

[75] D. Mondal and T. Nag, Finite-temperature dynamical quantum phase transition in a non-Hermitian system, Phys. Rev. B **107**, 184311 (2023).

[76] D. Mondal and T. Nag, Persistent anomaly in dynamical quantum phase transition in long-range non-Hermitian p-wave kitaev chain, Eur. Phys. J. B **97**, 59 (2024).

[77] A. Kosior and K. Sacha, Dynamical quantum phase transitions in discrete time crystals, Phys. Rev. A **97**, 053621 (2018).

[78] A. Kosior, A. Syrwid, and K. Sacha, Dynamical quantum phase transitions in systems with broken continuous time and space translation symmetries, Phys. Rev. A **98**, 023612 (2018).

[79] J. C. Halimeh, N. Yegovtsev, and V. Gurarie, Dynamical quantum phase transitions in many-body localized systems, arXiv:1903.03109.

[80] D. Trapin, J. C. Halimeh, and M. Heyl, Unconventional critical exponents at dynamical quantum phase transitions in a random Ising chain, Phys. Rev. B **104**, 115159 (2021).

[81] P. Jurcevic, H. Shen, P. Hauke, C. Maier, T. Brydges, C. Hempel, B. P. Lanyon, M. Heyl, R. Blatt, and C. F. Roos, Direct observation of dynamical quantum phase transitions in an interacting many-body system, Phys. Rev. Lett. **119**, 080501 (2017).

[82] N. Fläschner, D. Vogel, M. Tarnowski, B. S. Rem, D.-S. Lühmann, M. Heyl, J. C. Budich, L. Mathey, K. Sengstock, and C. Weitenberg, Observation of dynamical vortices after quenches in a system with topology, Nat. Phys. **14**, 265 (2018).

[83] X. Nie, B.-B. Wei, X. Chen, Z. Zhang, X. Zhao, C. Qiu, Y. Tian, Y. Ji, T. Xin, D. Lu, and J. Li, Experimental observation of equilibrium and dynamical quantum phase transitions via out-of-time-ordered correlators, Phys. Rev. Lett. **124**, 250601 (2020).

[84] M.A. Caprio, P. Cejnar, and F. Iachello, Excited state quantum phase transitions in many-body systems, Ann. Phys. **323**, 1106 (2008).

[85] P. Cejnar, P. Stránský, M. Macek, and M. Kloc, Excited-state quantum phase transitions, J. Phys. A: Math. Theor. **54**, 133001 (2021).

[86] A. Relaño, J. M. Arias, J. Dukelsky, J. E. García-Ramos, and P. Pérez-Fernández, Decoherence as a signature of an excited-state quantum phase transition, Phys. Rev. A **78**, 060102(R) (2008).

[87] P. Pérez-Fernández, A. Relaño, J. M. Arias, J. Dukelsky, and J. E. García-Ramos, Decoherence due to an excited-state quantum phase transition in a two-level Boson model, Phys. Rev. A **80**, 032111 (2009).

[88] P. Pérez-Fernández, P. Cejnar, J. M. Arias, J. Dukelsky, J. E. García-Ramos, and A. Relaño, Quantum quench influenced by an excited-state phase transition, Phys. Rev. A **83**, 033802 (2011).

[89] L. F. Santos and F. Pérez-Bernal, Structure of eigenstates and quench dynamics at an excited-state quantum phase transition, Phys. Rev. A **92**, 050101(R) (2015).

[90] C. M. Lóbez and A. Relaño, Entropy, chaos, and excited-state quantum phase transitions in the Dicke model, Phys. Rev. E **94**, 012140 (2016).

[91] F. Pérez-Bernal and L. F. Santos, Effects of excited state quantum phase transitions on system dynamics, Fortschr. Phys. **65**, 1600035 (2017).

[92] M. Kloc, P. Stránský, and P. Cejnar, Quantum quench dynamics in Dicke superradiance models, Phys. Rev. A **98**, 013836 (2018).

[93] W. Kopylov and T. Brandes, Time delayed control of excited state quantum phase transitions in the Lipkin–Meshkov–Glick model, New J. Phys. **17**, 103031 (2015).

[94] Q. Wang and H. T. Quan, Probing the excited-state quantum phase transition through statistics of Loschmidt echo and quantum work, Phys. Rev. E **96**, 032142 (2017).

[95] R. Puebla, A. Relaño, and J. Retamosa, Excited-state phase transition leading to symmetry-breaking steady states in the Dicke model, Phys. Rev. A **87**, 023819 (2013).

[96] R. Puebla and A. Relaño, Non-thermal excited-state quantum phase transitions, Europhys. Lett. **104**, 50007 (2013).

[97] V. M. Bastidas, P. Pérez-Fernández, M. Vogl, and T. Brandes, Quantum criticality and dynamical instability in the kicked-top model, Phys. Rev. Lett. **112**, 140408 (2014).

[98] R. Puebla and A. Relaño, Irreversible processes without energy dissipation in an isolated Lipkin-Meshkov-Glick model, Phys. Rev. E **92**, 012101 (2015).

[99] Q. Hummel, B. Geiger, J. D. Urbina, and K. Richter, Reversible quantum information spreading in many-body systems near criticality, Phys. Rev. Lett. **123**, 160401 (2019).

[100] Á. L. Corps and A. Relaño, Constant of motion identifying excited-state quantum phases, Phys. Rev. Lett. **127**, 130602 (2021).

[101] J. C. Halimeh, D. Trapin, M. Van Damme, and M. Heyl, Local measures of dynamical quantum phase transitions, Phys. Rev. B **104**, 075130 (2021).

[102] Y. Wu, Dynamical quantum phase transitions of quantum spin chains with a Loschmidt-rate critical exponent equal to $\frac{1}{2}$, Phys. Rev. B **101**, 064427 (2020).

[103] H. J. Lipkin, N. Meshkov, and A. J. Glick, Validity of many-body approximation methods for a solvable model: (i). exact solutions and perturbation theory, Nucl. Phys. **62**, 188 (1965).

[104] N. Meshkov, A. J. Glick, and H. J. Lipkin, Validity of many-body approximation methods for a solvable model: (ii). linearization procedures, Nucl. Phys. **62**, 199 (1965).

[105] A. J. Glick, H. J. Lipkin, and N. Meshkov, Validity of many-body approximation methods for a solvable model: (iii). diagram summations, Nucl. Phys. **62**, 211 (1965).

[106] P. Pérez-Fernández and A. Relaño, From thermal to excited-state quantum phase transition: The Dicke model, Phys. Rev. E **96**, 012121 (2017).

[107] Á. L. Corps and A. Relaño, General theory for discrete symmetry-breaking equilibrium states, arXiv:2303.18020.

[108] J. C. Halimeh, M. Van Damme, V. Zauner-Stauber, and L. Vanderstraeten, Quasiparticle origin of dynamical quantum phase transitions, Phys. Rev. Res. **2**, 033111 (2020).